Identification of a Rab GTPase-activating protein cascade that controls recycling of the Rab5 GTPase Vps21 from the vacuole

Meenakshi Rana, Jens Lachmann, and Christian Ungermann
Biochemistry Section, Department of Biology/Chemistry, University of Osnabrück, 49076 Osnabrück, Germany

ABSTRACT **Transport within the endocytic pathway depends on a consecutive function of the endosomal Rab5 and the late endosomal/lysosomal Rab7 GTPases to promote membrane recycling and fusion in the context of endosomal maturation. We previously identified the hexameric BLOC-1 complex as an effector of the yeast Rab5 Vps21, which also recruits the GTPase-activating protein (GAP) Msb3. This raises the question of when Vps21 is inactivated on endosomes. We provide evidence for a Rab cascade in which activation of the Rab7 homologue Ypt7 triggers inactivation of Vps21. We find that the guanine nucleotide exchange factor (GEF) of Ypt7 (the Mon1-Ccz1 complex) and BLOC-1 both localize to the same endosomes. Overexpression of Mon1-Ccz1, which generates additional Ypt7-GTP, or overexpression of activated Ypt7 promotes relocalization of Vps21 from endosomes to the endoplasmic reticulum (ER), which is indicative of Vps21 inactivation. This ER relocalization is prevented by loss of either BLOC-1 or Msb3, but it also occurs in mutants lacking endosome–vacuole fusion machinery such as the HOPS tethering complex, an effector of Ypt7. Importantly, BLOC-1 interacts with the HOPS on vacuoles, suggesting a direct Ypt7-dependent cross-talk. These data indicate that efficient Vps21 recycling requires both Ypt7 and endosome–vacuole fusion, thus suggesting extended control of a GAP cascade beyond Rab interactions.**

Monitoring Editor
Patrick J. Brennwald
University of North Carolina

Received: Feb 6, 2015
Revised: May 6, 2015
Accepted: May 6, 2015

INTRODUCTION

The endocytic pathway is a central route for delivering cargo from the plasma membrane via the endosome to the lysosome, where macromolecules are hydrolyzed into their respective monomers for recycling (Huotari and Helenius, 2011; Gautreau *et al.*, 2014). Its function depends on proteins and protein complexes that either generate vesicular carriers or promote their consumption at the target membrane. Within this pathway, the endosome serves as a sorting organelle that changes its morphology in the course of the endocytic pathway (Huotari and Helenius, 2011). Whereas early endosomes also promote recycling of selected receptors back to the plasma membrane and thus have tubular extensions, late endosomes are filled with intraluminal vesicles, which contain membrane proteins. This morphological change occurs in a maturation process that is accompanied by a change in the protein machinery, as seen with Rab GTPases: early endosomes carry Rab5 and late endosomes have Rab7 on their surface (Rink *et al.*, 2005; Poteryaev *et al.*, 2010). Rabs are switch-like GTP-binding proteins (Barr, 2013; Barr and Lambright, 2010; Hutagalung and Novick, 2011; Itzen and Goody, 2011; Lachmann *et al.*, 2011). In their inactive GDP form, Rabs are extracted from membranes by the guanine nucleotide dissociation inhibitor, which binds both the GTPase domain and the C-terminal prenyl anchor (Rak *et al.*, 2003). Guanine nucleotide exchange factors (GEFs) recruit the Rabs to their appropriate locations and convert them to the active GTP form, which can then bind to effectors such as tethering factors. Both active Rab5 and Rab7 bind to specific tethering factors to promote both recycling of receptors via tubular carriers and fusion with incoming vesicles.

This article was published online ahead of print in MBoC in Press (http://www.molbiolcell.org/cgi/doi/10.1091/mbc.E15-02-0062) on May 13, 2015.

Address correspondence to: Christian Ungermann (cu@uos.de); www.biochemie.uni-osnabrueck.de.

Abbreviations used: BSA, bovine serum albumin; DOGS-NTA, 1,2-dioleoyl-*sn*-glycero-3-[(*N*-(5-amino-1-carboxypentyl) imino-diacetic acid)succinyl]; ER, endoplasmic reticulum; GAP, GTPase-activating protein; GEF, guanine nucleotide exchange factor; GFP, green fluorescent protein; GST, glutathione *S*-transferase; MLV, multilamellar vesicle; TAP, tandem affinity purification; YFP, yellow fluorescent protein.

We have characterized this pathway in yeast and analyzed the CORVET complex as an effector of the Rab5-like Vps21 and the HOPS complex as a Ypt7 effector (Bröcker *et al.*, 2012; Balderhaar and Ungermann, 2013; Balderhaar *et al.*, 2013). Moreover, we have shown that localization of the Ypt7 GEF, which we identified as the Mon1-Ccz1 complex (Nordmann *et al.*, 2010; Cabrera *et al.*, 2014), depends on Vps21 and endosomal fusion factors (Cabrera *et al.*, 2013). As HOPS is required for the final fusion between late endosomes and the lysosome-like vacuole (Seals *et al.*, 2000; Wurmser *et al.*, 2000), we reasoned that Ypt7 activation and Vps21 inactivation must be coordinated. Such counterregulation between Rabs that act in consecutive reactions on organelles or vesicles have been termed a Rab cascade, wherein the activation of one Rab by a specific GEF triggers the inactivation of the previously acting Rab (del Conte-Zerial *et al.*, 2008; Hutagalung and Novick, 2011; Barr, 2013). A Rab GTPase-activating protein (GAP) cascade could function such that the activated Rab recruits the previous GAP by direct interaction, as described for intra-Golgi transport in yeast (Rivera-Molina and Novick, 2009; Suda *et al.*, 2013).

For the endocytic pathway, we previously identified the hexameric BLOC-1 complex as a regulator of the Rab5-like Vps21 on endosomes (John Peter *et al.*, 2013). In metazoan cells, BLOC-1 exists as an octameric elongated complex that has been detected on tubular endosomal extensions and is involved in the biogenesis of lysosome-related organelles (Di Pietro *et al.*, 2006; Salazar *et al.*, 2006; Setty *et al.*, 2007; Lee *et al.*, 2012). We showed that yeast BLOC-1 binds to Vps21-GTP and recruits the GAP Msb3 to endosomes (John Peter *et al.*, 2013); it also controls the exocytic Rab Sec4 at the plasma membrane (Gao *et al.*, 2003). Consequently loss of BLOC-1 or Msb3 sorted Vps21 to the vacuole membrane (Lachmann *et al.*, 2012; Nickerson *et al.*, 2012; John Peter *et al.*, 2013). Similarly, Vps21 was mislocalized to the vacuole surface in a mutant of Msb3 that lost its GAP activity (John Peter *et al.*, 2013).

Msb3 is a strong GAP for Vps21, but it can also act on Ypt7 and thus affect vacuole fusion (Lachmann *et al.*, 2012; Nickerson *et al.*, 2012). We reasoned that the activity of Msb3 on Vps21 must be regulated by its BLOC-1–dependent recruitment and the availability of Ypt7 and thus analyzed the cross-talk between Ypt7, BLOC-1, and Vps21. Our data now provide evidence that active Ypt7 promotes inactivation and recycling of Vps21, in agreement with an endocytic Rab GAP cascade.

RESULTS

Dissection of the interfaces between BLOC-1, Msb3, and Vps21

Yeast BLOC-1 provides an intriguing link between a Rab (Vps21) and its own GAP (Msb3). To understand the control of Vps21 inactivation at the late endosome, we began to explore the molecular interactions between BLOC-1, Vps21, and Msb3. To find the specific subunits of BLOC-1 that act as binding partners for Vps21 and Msb3, we initially used the split–yellow fluorescent protein (YFP) assay, in which the two proteins are tagged with the C-terminal VC-half (C-terminal half of YFP) and N-terminal VN-half (N-terminal half of YFP). Previously we detected interaction of Bli1, Cnl1, Snn1, and Kxd1 with Msb3 (John Peter *et al.*, 2013), and we observed here a clear in vivo interaction of Vps21 with all BLOC-1 subunits except Bls1, presumably at the endosome (Figure 1A). As BLOC-1 is a hexameric complex made up of small subunits, this technique is not suitable to identify the specific interactor. We thus used purified BLOC-1 subunits (except for Bls1, which was insoluble) for in vitro interaction with purified Msb3 and detected Bli1 as a specific binding partner for Msb3 (Figure 1B). A similar approach was applied to find the specific subunit of BLOC-1 that interacts with active Vps21. For this, we added purified BLOC-1 subunits to glutathione *S*-transferase (GST)-Vps21 and GST-Ypt7 that were preloaded with GTPγS or GDP. Unfortunately, none of the tested single BLOC-1 subunits showed an interaction with Vps21-GTPγS, whereas the hexameric BLOC-1 purified from yeast did as shown before (Figure 1, C and D; John Peter *et al.*, 2013). We cannot yet distinguish whether BLOC-1 needs to be hexameric to bind Vps21 or whether a combination of two or more proteins is required to interact with Vps21. To determine the subunit interactions within BLOC-1, we incubated purified GST-tagged subunits with selected His-tagged subunits and probed the eluate with His-specific antibodies. We observed strong interactions of GST-Vab2 with Bli1 and Snn1 (Figure 1E), of GST-Snn1 with Bli1, and of GST-Kxd1 with Cnl1 (Figure 1F). Some Cnl1 was also recovered with GST-Bli1 (Figure 1G). Based on these observations, we generated a putative interaction map of BLOC-1 that suggests a linear arrangement, similar to the previously suggested arrangement for metazoan BLOC-1 (Lee *et al.*, 2012). The Bls1 interactions are based on previous interaction studies summarized by Levine and coworkers (Hayes *et al.*, 2011).

Reconstitution of Msb3 GAP activity in the presence of BLOC-1

The BLOC-1 complex recruits Msb3 to endosomes in vivo. We asked whether, in addition to this function, BLOC-1 also modulates Msb3 GAP activity on Vps21 to provide spatiotemporal control during endosomal maturation. We therefore used a radioactive GTP hydrolysis assay. Recombinant Msb3 acts as a potent GAP toward Vps21 in vitro (Lachmann *et al.*, 2012; Nickerson *et al.*, 2012; Figure 2A). We titrated the purified BLOC-1 complex into the GAP assay but did not observe any alteration of GAP activity of Msb3 toward Vps21 (Figure 2B). Because GAPs promote GTP hydrolysis of membrane-bound Rab GTPases, we tried to mimic this scenario in vitro. For this, we used C-terminally hexa-His-tagged Vps21 that was preloaded with γ-[^{32}P] GTP and immobilized it on the surface of multilamellar vesicles (MLVs) containing DOGS-NTA (1,2-dioleoyl-*sn*-glycero-3-[(*N*-(5-amino-1-carboxypentyl) imino-diacetic acid) succinyl]) lipids. Msb3 strongly promoted GTP hydrolysis of membrane-bound Vps21 in comparison with Vps21 in solution with up to 50-fold increased activity (Figure 2C). Notably, it was the membrane-bound Vps21 causing this increased activity, because the GAP activity was almost similar if MLVs without the DOGS-NTA lipid were used (Figure 2C). Because purified BLOC-1 promoted strong GTP hydrolysis even in the absence of additional Msb3, we speculated that BLOC-1 might have been copurified with trace amounts of Msb3 from yeast cells. To test this, we purified BLOC-1 from an *msb3*Δ strain and compared the GTP hydrolysis on Vps21 with BLOC-1 purified from a wild-type strain. Indeed, BLOC-1 purified from an *msb3*Δ strain was now silent in the GAP assay (Figure 2D). However, this BLOC-1 strain still did not affect GAP activity when added in excess into the assay (Figure 2E). Because Msb3 purified from either yeast or *Escherichia coli* is rather sticky and interacts with membranes even without BLOC-1 addition, it might not require BLOC-1 to efficiently inactivate Vps21 in vitro. The lack of regulation also precluded any further analysis of possible regulators.

BLOC-1 and Mon1-Ccz1 colocalize at the endosomes

As our data did not yet clarify how BLOC-1 and Msb3 might cooperate to control Vps21 activity on membranes, we turned to in vivo analyses. During the transition of early endosomes to late endosomes and vacuoles, Ypt7 replaces Vps21, likely similar to observations made in metazoan cells (Rink *et al.*, 2005; Poteryaev *et al.*,

2010). We hypothesized that the activation of Ypt7 by the Mon1-Ccz1 GEF complex and inactivation of Vps21 by Msb3 should be coordinated on endosomes. To analyze the possible cross-talk, we analyzed the localization pattern of early and late endosomal components involved in Rab control. We observed that all the BLOC-1 subunits (tagged with C-terminal green fluorescent protein [GFP]) and Vps21 colocalized with Mon1, with up to 75% overlap between Mon1 and the BLOC-1 subunit Snn1 (Figure 3, A and B). This colocalization of BLOC-1 and Mon1-Ccz1 was not interdependent, as Ccz1 localized to endosomes without BLOC-1 (Figure 3C). Also, the location of Ypt7 was unaffected by deletion of the BLOC-1 subunit Kxd1, further confirming that *bloc-1* deletion has no effect on the location and functionality of Mon1-Ccz1 (Figure 3D), and BLOC-1 remained endosomal without the Mon1-Ccz1 complex (Figure 3, E and F). We also tried to localize Ypt7 relative to BLOC-1 and Vps21 but could not resolve late endosomes and vacuoles at this resolution (Figure 3, G and H).

Mon1-Ccz1 negatively regulates Vps21 activation

In *Caenorhabditis elegans*, SAND-1/Mon1 acts as a crucial factor for the Rab5 to Rab7 transition by displacing the Rab5 GEF, Rabex-5, from endosomes (Poteryaev *et al.*, 2010), even though plant cells do not require Rab7 activation for endosomal maturation (Singh *et al.*, 2014). When we analyzed Vps21-positive structures, we observed that the number of GFP-Vps21–positive structures almost doubled in the *mon1*Δ *ccz1*Δ strain compared with wild-type (Figure 4, A and C–E). Moreover, the increased number of Vps21-positve structures is accessible by FM4-64 stain (Figure 4E), which confirms that these are indeed endosomal structures. We also counted the Vps8-positive endosomal structures in both the strains but observed no difference (Figure 4, B–D). In agreement with this, coexpression of Vps8, tagged with mCherry, and GFP-Vps21 resulted in more Vps21-positive dots in the *mon1*Δ *ccz1*Δ background (Figure 4C). It is possible that Mon1-Ccz1 has some role in the inactivation of Vps21, as in mammalian cells, and thus more Vps21 is observed in membranes, which may be bound to other effectors, such as Vac1, Vps34, or BLOC-1, in addition to Vps8. To test this further, we cooverexpressed Mon1-Ccz1 and localized Vps21, which now accumulated on ER membranes, marked by Sec63-MARS (Figure 4F). We previously showed that GEF inactivation results in mislocalization of the corresponding Rab to the ER (Cabrera and Ungermann, 2013; Auffarth *et al.*, 2014), in agreement with previous data (Ali *et al.*, 2004). To analyze whether the mislocalization of Vps21 to the ER under these conditions is due to the Mon1-Ccz1 amount or to the more active Ypt7, we deleted *ypt7* in the same strain background. Under these conditions, Vps21 remained on vesicles and vacuolar membranes (Figure 4G). The similar localization pattern for Vps21 was observed even upon deletion of *ypt7* in wild-type cells (Figure 4H), suggesting that Ypt7 itself is required for Vps21 inactivation.

Activated Ypt7 signals for Vps21 inactivation via BLOC-1 and Msb3

To address the possible connection between Ypt7 activation and Vps21 inactivation, we overexpressed Ypt7 and then monitored Vps21 localization. Overexpression of wild-type Ypt7 did not affect Vps21 localization to endosomal dots (Figure 5B). However, when GTP-locked Ypt7 Q68L was overexpressed, Vps21 was mainly found on the ER membrane (Figure 5C). This localization was rescued by cooverexpression of the Vps21 GEF protein, Vps9 (Figure 5D), indicating that the ER localization of Vps21 reflects its inactivation under these conditions (Cabrera and Ungermann, 2013). In contrast, upon deletion of *msb3* or *kxd1*, Vps21 remained bound to the vacuole membrane (Figure 5, E and F), indicating that Ypt7-mediated inactivation requires Msb3 and BLOC-1.

To find further support for this model, we generated a strain lacking both the GEF Mon1-Ccz1 and Msb3 and complemented this with a fast-cycling Ypt7 (K127E) mutant that bypasses Mon1-Ccz1 function (Kucharczyk *et al.*, 2001; Cabrera and Ungermann, 2013). Consequently vacuoles were round, and Vps21 localized to endosomal dots (Figure 5K). In the absence of Msb3, however, Vps21 localized to the vacuole membrane (Figure 5N), suggesting that it is indeed active Ypt7 that is required for efficient Vps21 inactivation and recycling.

Fusion machinery is essential for Vps21 inactivation

We next asked whether Ypt7 acts directly on Vps21 or requires other downstream effectors. Previously the retromer subunit Vps35 and the HOPS subunits Vps41 and Vps39 have been described as Ypt7 effectors (Rojas *et al.*, 2008; Balderhaar *et al.*, 2010; Ostrowicz *et al.*, 2010; Plemel *et al.*, 2011; Bröcker *et al.*, 2012). Furthermore, Yck3 phosphorylates the HOPS subunit Vps41 and thus affects trafficking to the vacuole (LaGrassa and Ungermann, 2005; Cabrera *et al.*, 2010). We therefore monitored Vps21 localization upon Ypt7 Q68L overproduction upon deletion of either *vps35* or *yck3* and observed the same ER localization as before (Figure 6, A and B), indicating that neither Vps41 phosphorylation nor retromer are involved in the inactivation of Vps21.

In contrast, when any fusion factor directly involved in endosome–vacuole fusion, such as the HOPS subunit Vps41 or the SNAREs (soluble *N*-ethylmaleimide–sensitive fusion protein receptors) Vam3 or Vam7, was deleted, Vps21 accumulated on endosomes and fragmented vacuoles (Figure 6, C–E). A similar effect was also seen with Ypt7 overexpression (Figure 6, F–H), which in the wild-type background promotes ER localization of Vps21 (Figure 5C). This indicates that the inactivation of Vps21 via BLOC-1 and Msb3 requires either fusion with the vacuole or the recruitment of the vacuole fusion machinery.

BLOC-1 interacts with Ypt7 and HOPS

To analyze the cross-talk of BLOC-1 with Ypt7 and the fusion machinery, we tested for direct interactions. As we could not identify a specific interaction between BLOC-1 and Ypt7 using Rab pull-down assays, we turned to the split-YFP assay, as explained in Figure 1. When VN-Ypt7 and Kxd1-VC were coexpressed in wild-type cells, no signal could be detected (Figure 7A). Our data suggest that active Ypt7 interacts with BLOC-1, and afterward, BLOC-1 recruits Msb3 to inactivate Vps21. Hence the interaction between BLOC-1 and Ypt7 should be stabilized in an *msb3* deletion. Indeed, we observed a clear signal on vacuoles in *msb3*Δ cells, indicating that Kxd1 and Ypt7 interact under these conditions (Figure 7B). We also showed that Ypt7 and the fusion machinery might promote BLOC-1/Msb3–mediated recycling of Vps21, and we therefore tested for interaction of BLOC-1 with the HOPS complex by the same approach. Indeed, the Rab-specific HOPS subunits Vps39 and Vps41 showed interaction with BLOC-1 subunits by the split-YFP approach (Figure 7, C and D). Interestingly, strong signals were observed in single dots proximal to the vacuole. To test whether such dots were endosomes, we coexpressed mCherry-tagged Vps21 with VN-Vps41 and two VC-tagged BLOC-1 subunits (Figure 7, E and F) and observed strong colocalization in both cases. We then incubated BLOC-1 purified from an *msb3*Δ strain with purified HOPS or AP-3 complex, which were previously immobilized via FLAG-tag (unpublished data). BLOC-1 was specifically retained on HOPS, whereas the much more abundant AP-3

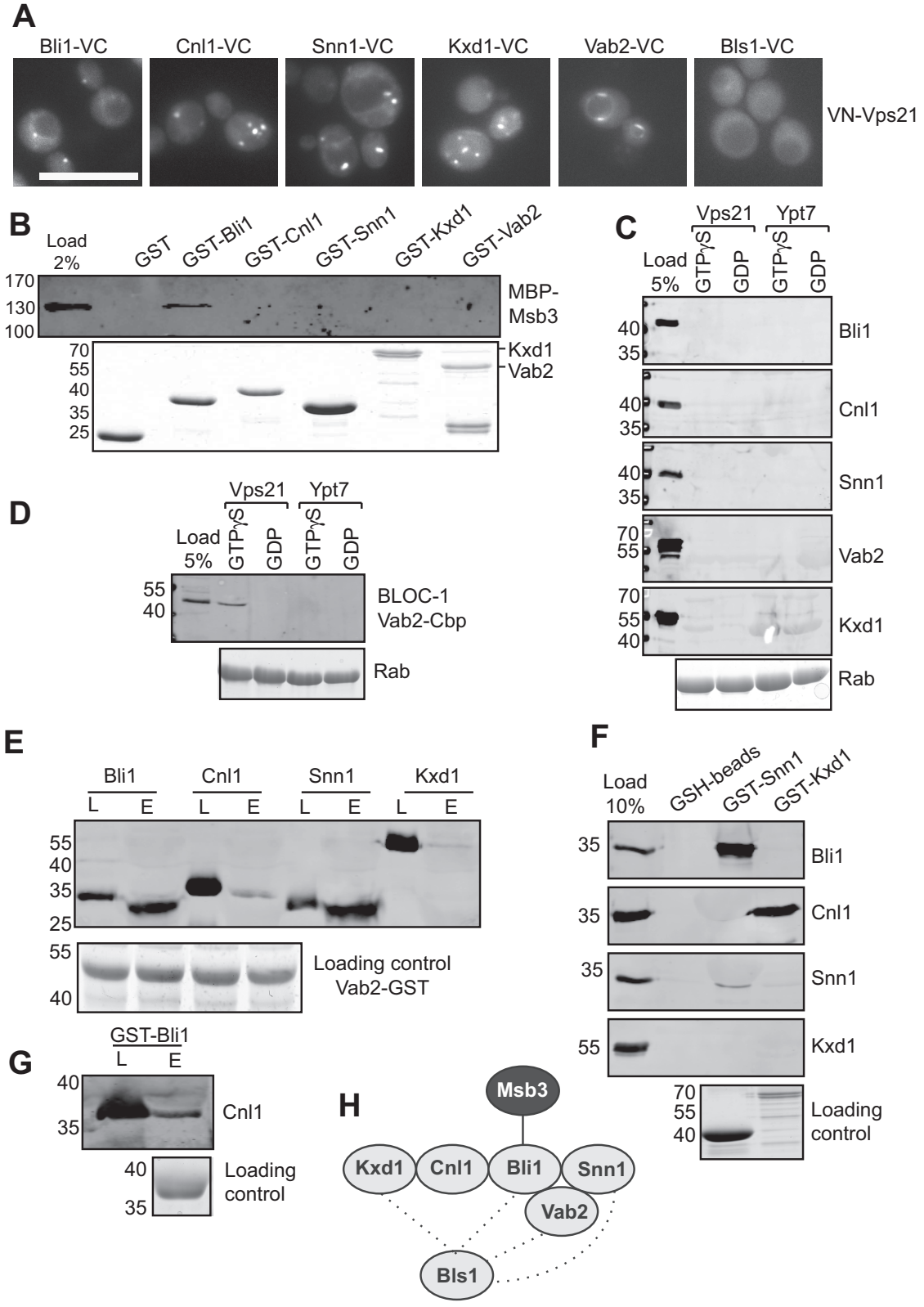

FIGURE 1: Dissection of the interfaces between BLOC-1, Vps21, and Msb3. (A) BLOC-1 subunits (except Bls1) interact with Vps21 in vivo. C-terminally VC-tagged BLOC-1 subunits were coexpressed with VN-Vps21 and analyzed by fluorescence microscopy. Scale bar: 10 μm. (B) Bli1 binds to purified MBP-Msb3 in vitro. Purified BLOC-1 subunits GST-Bli1, GST-Cnl1, GST-Snn1, GST-Vab2, and GST-Kxd1 were coupled to glutathione beads individually and incubated with purified MBP (maltose-binding protein)-Msb3. The bound protein was eluted by boiling and detected by Western blotting with antibodies against MBP. Glutathione beads coupled to GST were used as a negative control. (C and D) Individual BLOC-1 subunits are not sufficient to bind to Vps21-GTP. Recombinant GST-Vps21 and GST-Ypt7 were preloaded with GTPγS and

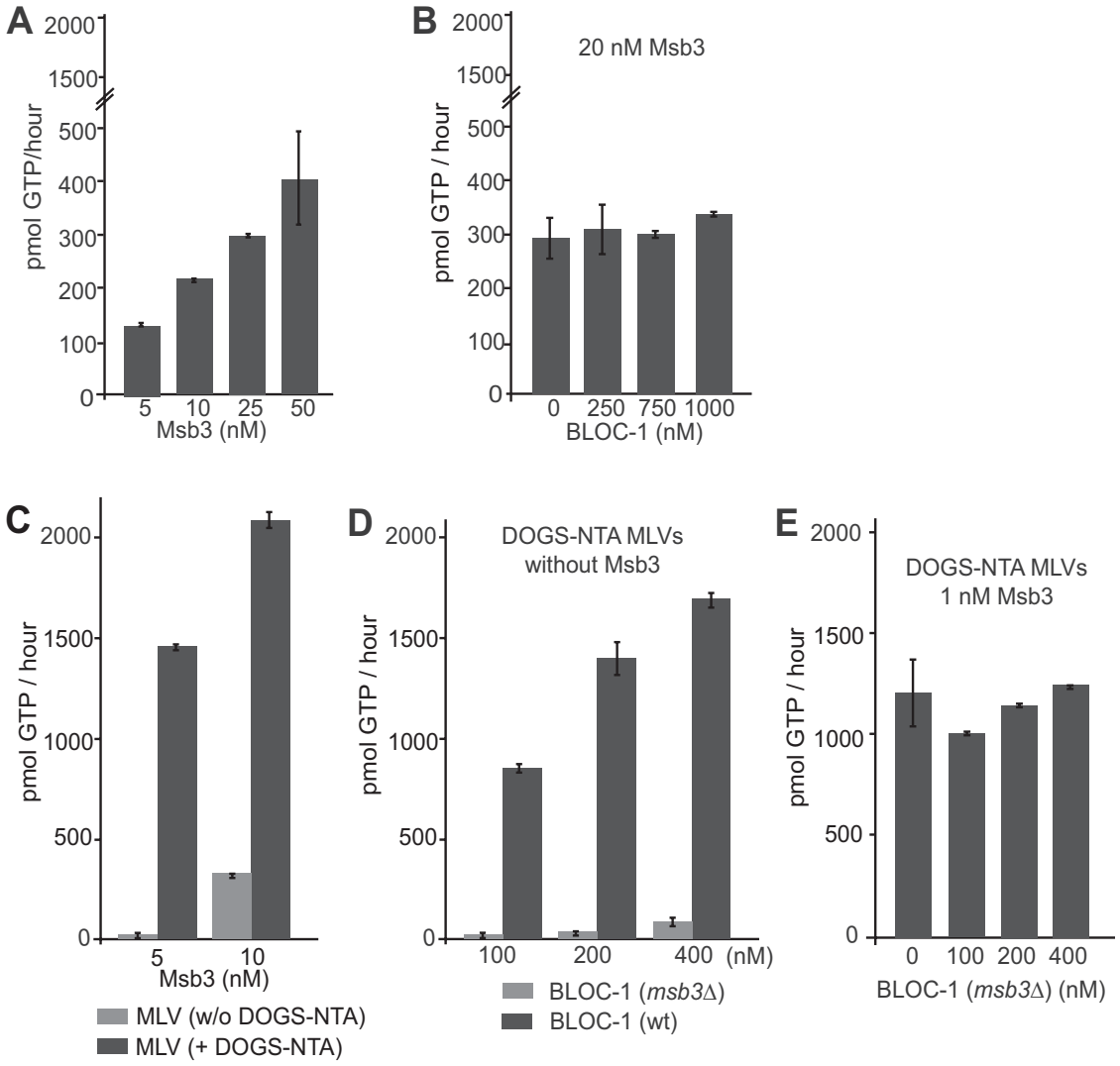

FIGURE 2: Reconstitution of GAP activity with BLOC-1 and Msb3. (A) Titration of Msb3 to GAP assay with Vps21. Vps21-His (1 µM) was preloaded with γ-[^{32}P] GTP, and the rate of GTP hydrolysis was measured by following released ^{32}P upon addition of indicated proteins. Purified Msb3 was added at the indicated concentrations. (B) Influence of purified BLOC-1 on Msb3-mediated GAP activity in solution. BLOC-1 was added at the indicated concentrations to the GAP assay with Vps21, driven by 20 nM Msb3. (C) Msb3 activity increases dramatically on membrane-bound Vps21. Preloaded Vps21-His was incubated with different concentrations of Msb3 and MLVs (0.5 mM) with (black bars) or without (gray bars) DOGS-NTA. (D) Msb3 is copurified with BLOC-1. Overexpressed BLOC-1 was purified from wild-type or *msb3*Δ cells, and added in the indicated concentrations to liposomes carrying DOGS-NTA as in C. (E) Effect of BLOC-1 on Msb3-mediated GAP activity. The indicated concentrations of BLOC-1 from *msb3*Δ cells was added to the GAP assay in the presence of MLVs with DOGS-NTA, 1 nM Msb3, and 1 µM loaded Vps21. Experiments were done at least three times. Representative experiments with duplicated samples are shown.

complex showed only weak binding (Figure 7G). These data suggest that BLOC-1 interacts with Ypt7 and HOPS at the endovacuolar interface, likely as a prerequisite of Vps21 inactivation here or at the vacuole membrane.

DISCUSSION

Within this study, we provide support for a Rab GAP cascade wherein the effector of the downstream Rab is involved in controlling Vps21 levels at the endosome (Figure 7H). We show that Msb3 is closely

GDP and then coupled to the GSH beads. These were then incubated with purified His-SUMO–tagged BLOC-1 subunits (C) or purified BLOC-1 complex purified from yeast (John Peter *et al.*, 2013). The bound proteins were eluted with EDTA, and the interaction was detected by Western blotting with anti-His and anti-TAP antibodies. (E–G) Identification of BLOC-1 interactions. N-terminally His-SUMO (HS)-tagged recombinant BLOC-1 subunits (HS-Bli1, HS-Cnl1, HS-Snn1, HS-Kxd1, HS-Vab2) were purified and incubated for 2 h at 4°C with immobilized Vab2-GST (E), GST-Snn1 and GST-Kxd1 (F), and GST-Bli1 (G). The bound subunits were analyzed by Western blotting after elution from the beads. L, 10% of load; E, 75% of eluate. (H) Proposed subunit arrangement of BLOC-1 complex. Because Bls1 could not be purified, dashed lines show previously reported interactions of Bls1 with other BLOC-1 subunits (Hayes *et al.*, 2011).

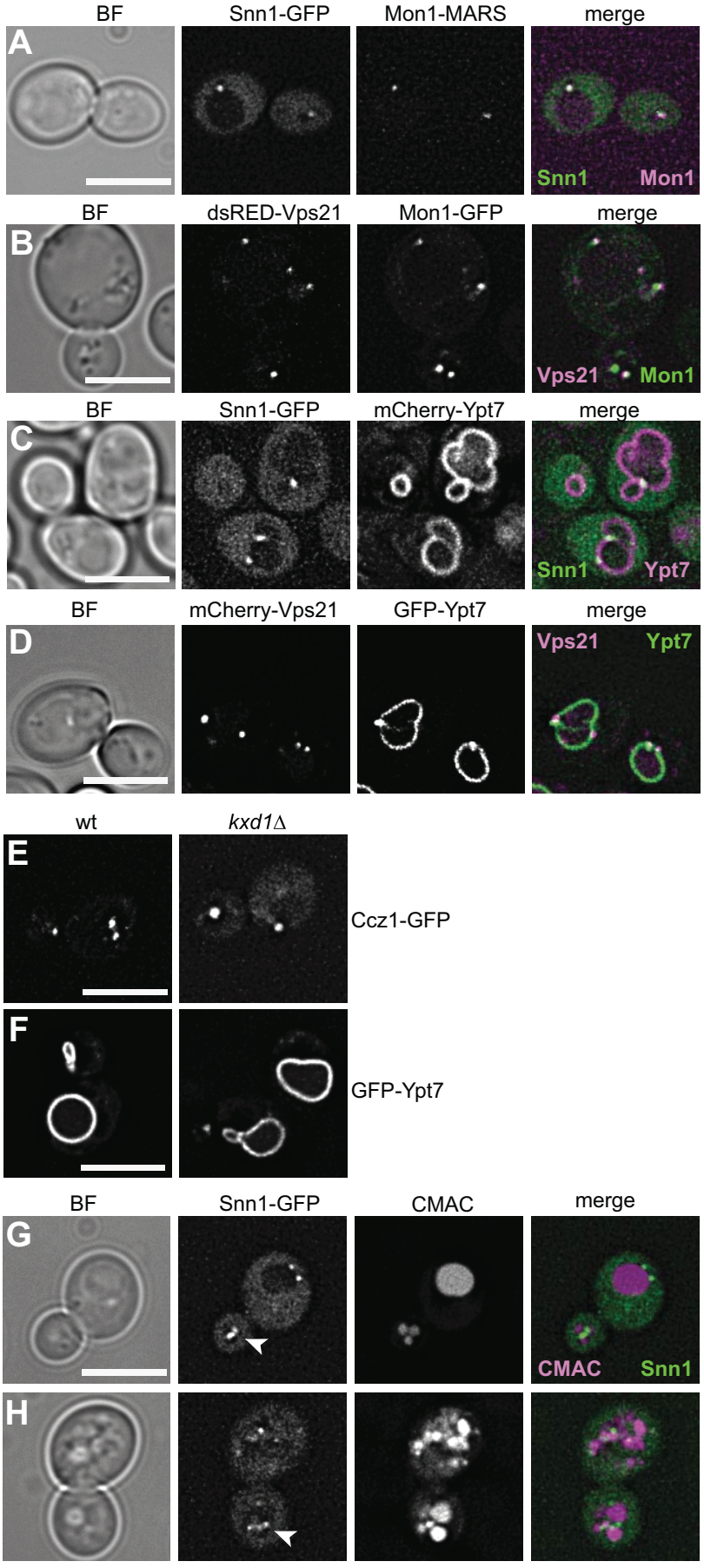

associated with BLOC-1 and can inactivate Vps21 efficiently on liposomes. Even though Msb3 activity on Vps21 was not modulated by BLOC-1 in vitro, this cross-talk was revealed in vivo. We show here that Mon1-Ccz1 and BLOC-1 colocalize in 75% of all analyzed endosomes and reveal that Mon1-Ccz1–mediated activation of Ypt7 promotes efficient release of Vps21 from endosomes. As has been shown previously for other Rabs (Cabrera and Ungermann, 2013), Vps21 then accumulates at the ER. Our data further show that efficient release of Vps21 requires BLOC-1 and Msb3, Ypt7-GTP, and fusion with the vacuole (Figure 7H). Of note, isolated Vps21 also has some intrinsic hydrolytic activity, which could explain its partial redistribution to endosomes, even in the absence of Msb3 (Lachmann *et al.*, 2012; Nickerson *et al.*, 2012). Deletions in the SNAREs Vam3 and Vam7 as well as the HOPS Vps41 subunit prevented release of Vps21 (Figure 6). We thus consider it likely that the BLOC-1 complex, and possibly Msb3, respond to both Ypt7-GTP and its effector proteins and possibly to the change in membrane composition due to endosome–vacuole fusion. In support of this, we observed an interaction of BLOC-1 and Ypt7 on the vacuole if Msb3 had been deleted, and we detected interactions of BLOC-1 and the Rab-specific HOPS subunits Vps39 and Vps41 on vacuoles and endosomes (Figure 7). Interestingly, the absence of HOPS-specific subunits results in increased colocalization of Rab5 and Rab7 (Solinger and Spang, 2014), similar to our observations on Vps21 when HOPS subunits were deleted (Figure 6), suggesting that the mechanism on Rab5/Vps21 turnover is conserved.

FIGURE 3: Cross-talk between BLOC-1 and the Ypt7 GEF, Mon1-Ccz1. (A) BLOC-1 and Mon1-Ccz1 strongly colocalize. Snn1-GFP was coexpressed with Mon1-MARS, and the cells were visualized by fluorescence microscopy. Scale bar: 5 μm. Of the Mon1-MARS–positive endosomes, 75.5% colocalized with Snn1-GFP. In total, 100 cells were used for the calculation. Scale bar: 5 μm. (B) Vps21 colocalizes with Mon1-Ccz1. dsRED-Vps21 and Mon1-GFP were coexpressed and visualized as in A. (C and D) Mon1-Ccz1 does not require BLOC-1 for endosomal recruitment. Ccz1-GFP (C) and GFP-Ypt7 (D) were localized in wild-type and *kxd1*Δ strains. (E and F) BLOC-1 does not require Mon1-Ccz1 for endosomal recruitment. Snn1-GFP was localized in wild-type and *mon1*Δ *ccz1*Δ strains. Arrowheads indicate Snn1-GFP–positive sites. (G) Localization of BLOC-1 relative to Ypt7. Snn1-GFP was coexpressed with mCherry-Ypt7. (H) Relative localization of Vps21 and Ypt7 in wild-type cells. mCherry-Vps21 and GFP-Ypt7 were coexpressed and analyzed by fluorescence microscopy.

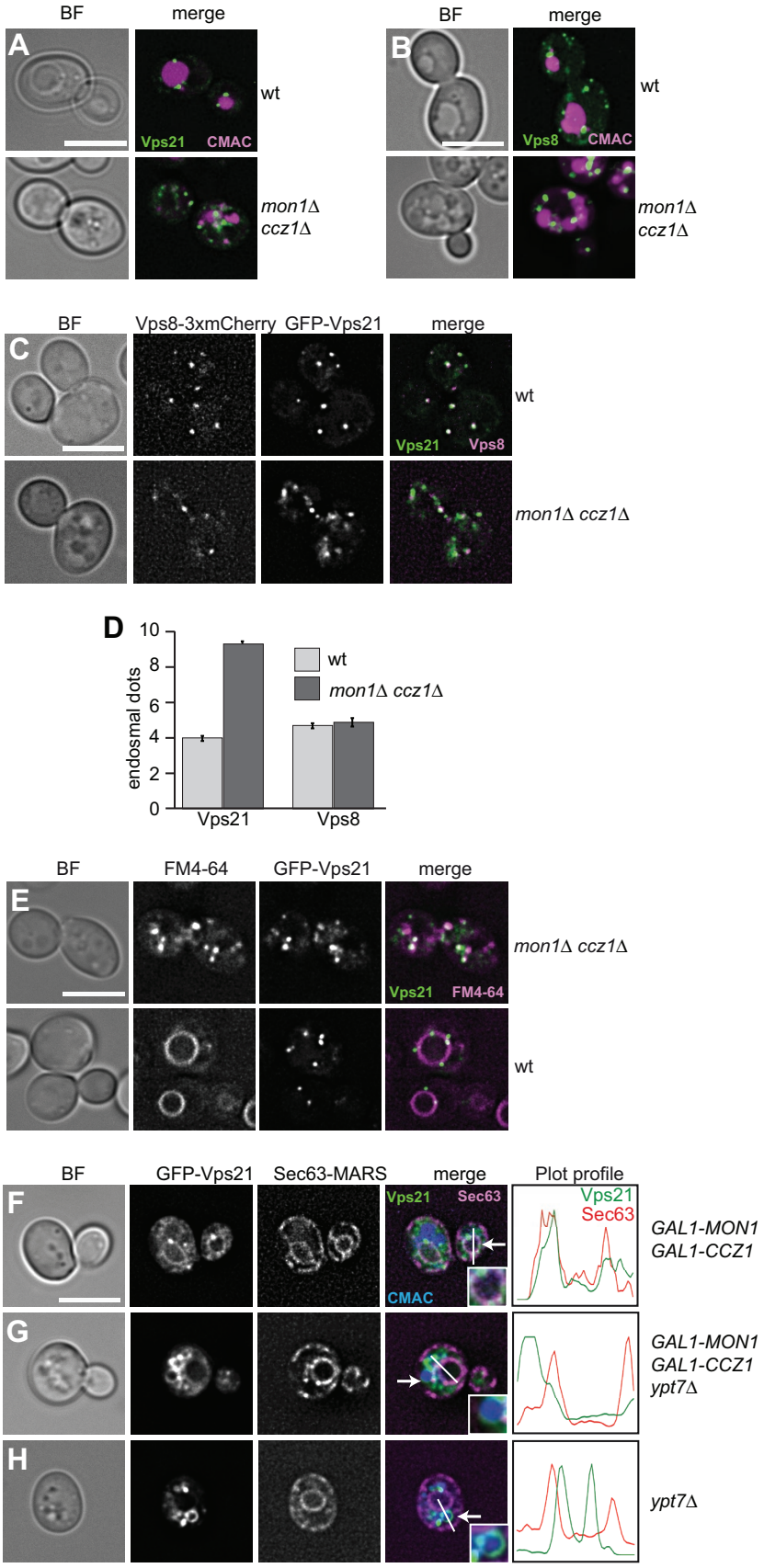

FIGURE 4: Mon1-Ccz1 negatively regulates Vps21 activation. (A–E) Vps21-positive endosomal number increases in the absence of the Ypt7 GEF complex. The localization of GFP-Vps21 (A) and Vps8-GFP (B) was analyzed in wild-type and *mon1*Δ *ccz1*Δ double deletion strains. Vacuoles are stained with CMAC. In C Vps8-3xmCherry and GFP-Vps21 were coexpressed. (D) Vps21- and Vps8-positive dots were counted in wild-type and *mon1*Δ *ccz1*Δ cells by using a self-made plug-in for ImageJ (Arlt *et al.*, 2015a). The bars represent the average number calculated from 50 cells in the indicated strains. The error bars represent the SEM. (E) The increased Vps21-positive dots in *mon1*Δ *ccz1*Δ cells are endosomes. GFP-Vps21–expressing wild-type and *mon1*Δ *ccz1*Δ cells were labeled with FM4-64 dye and monitored after 20 min. (F–H) Mon1-Ccz1 and Ypt7 promote inactivation of Vps21. GFP-Vps21 and Sec63-MARS were coexpressed in the indicated strains; the vacuolar lumen was stained with CMAC. The cells were grown in YPG medium to induce the expression of the Mon1-Ccz1 complex, which is under the control of the *GAL1*-promoter (F and G) (Nordmann *et al.*, 2010), and analyzed by fluorescence microscopy. The plot profile represents the colocalization between GFP-Vps21 and Sec63-MARS along the indicated line. The arrowheads represent the area of inset. Scale bar: 5 μm.

The connection between the activation of Ypt7 and the inactivation of Vps21 provide a new example of a Rab GAP cascade that includes the effector downstream of the next Rab. At present, we do not yet understand how this cross-talk is mediated at the molecular level. The initial recruitment of BLOC-1 and thus the associated Msb3 is Vps21 dependent, though Msb3 is likely not yet active (John Peter al., 2013). Both Vps21-GTP and Ypt7-GTP are substrates of Msb3 (Lachmann *et al.*, 2012; Nickerson *et al.*, 2012), even though only Vps21 seems to be inactivated at the endosome or upon arriving at the vacuole (John Peter *et al.*, 2013). Potentially, BLOC-1 is required not only to recruit Msb3 to endosomes but also to target Msb3 specifically to Vps21 during endosome maturation and fusion, and Msb3 might become active only if Ypt7-GTP becomes available and promotes fusion. In agreement with this, both *ypt7*Δ and *msb3*Δ cause relocalization of Vps21 to vacuole-like structures (Figures 4H and 5H; John Peter *et al.*, 2013).

Because the yeast GAP proteins identified show promiscuous GAP activity for multiple Rabs in vitro, such kind of control by BLOC-1 seems plausible. On vacuoles, Msb3 also seems to target available Ypt7-GTP (Lachmann *et al.*, 2012; Nickerson *et al.*, 2012) and may thus sharpen the effect of GEF-mediated activation of Ypt7. Our observations are also in line with the "cutout switch" model proposed by Zerial and coworkers for Rab5 to Rab7 conversion in endosomal maturation (del Conte-Zerial *et al.*, 2008). This model argues that Rab5 activates Rab7 up to a threshold level, after

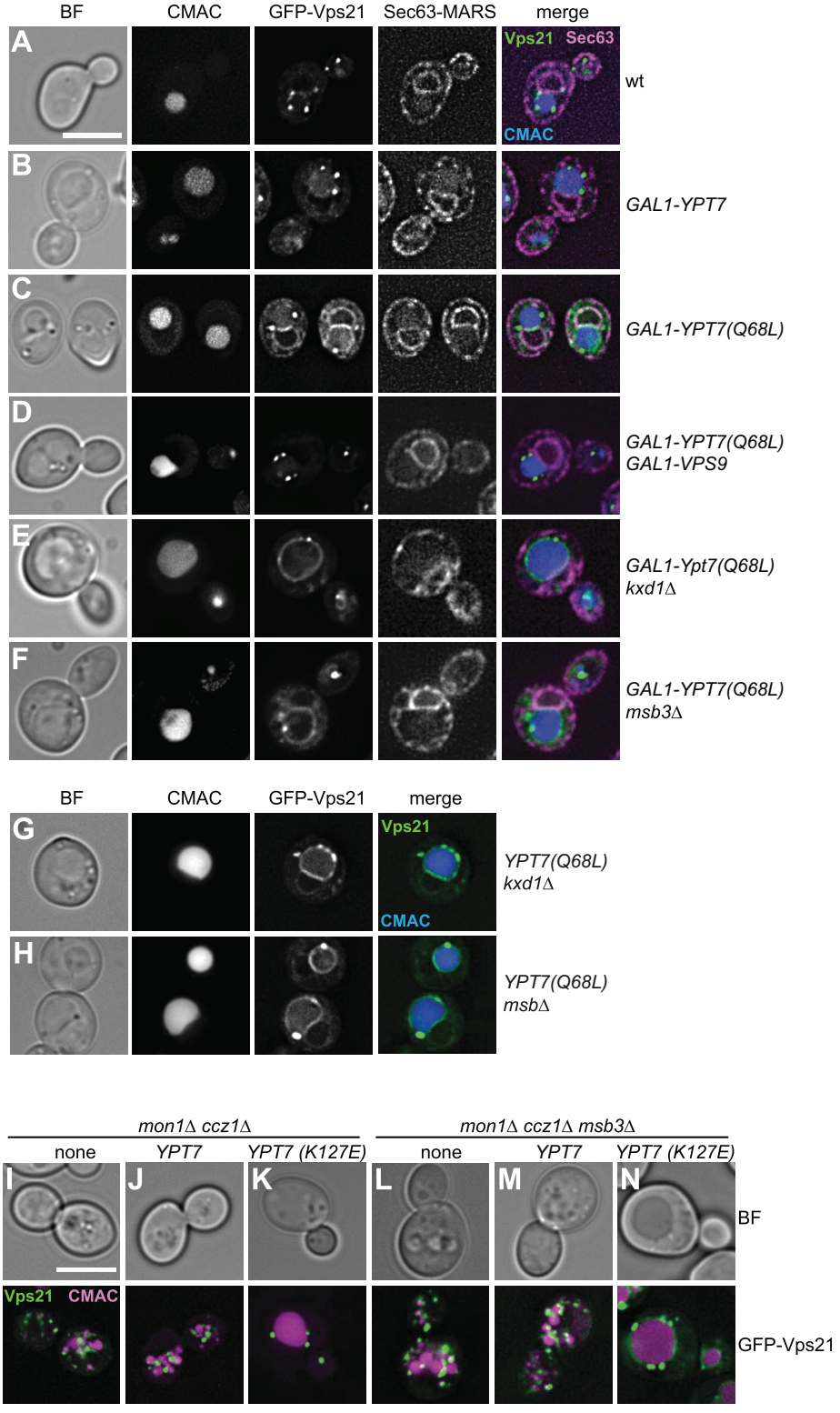

FIGURE 5: Activated Ypt7 promotes the inactivation of Vps21 via BLOC-1 and Msb3. (A–F) Effect of Ypt7 overexpression on Vps21 localization. GFP-Vps21 and Sec63-MARS were coexpressed in the indicated strains; the vacuolar lumen was stained with CMAC. The cells were grown in YPG medium to induce the expression of *GAL1* promoter and analyzed by fluorescence microscopy. (A) Wild-type cells, (B) overexpression of Ypt7, (C–F) overexpression of GTP-locked Ypt7 Q68L, (D) cooverexpression of the Vps21 GEF Vps9, (E and F) deletion of *kxd1* and *msb3* upon Ypt7 (Q68L) overexpression. (G and H) Deletion of *kxd1* and *msb3* in cells harboring Ypt7 Q68L under the endogenous promoter is shown as a control. Scale bar: 5 μm. (I–N) Effect of a fast-cycling Ypt7 mutant on Vps21 localization. GFP-Vps21 was visualized in the indicated strains expressing no plasmid or plasmids encoding wild-type Ypt7 or Ypt7 (K127E). Vacuoles are stained with CMAC. Scale bar: 5 μm.

which Rab7 inactivates Rab5 by a negative-feedback mechanism. Similar models that take GAP- and GEF-controlled activity into account have been proposed for Rabs in general (Barr, 2013). In this study, we also show that active Ypt7 signals for the inactivation and further displacement of Vps21 from endosomes. When Ypt7 or fusion is impaired, Vps21 accumulates in larger endosomal structures. However, our data suggest that it is not the Rab itself, but rather the associated machinery, that triggers inactivation.

Interestingly, the late-Golgi yeast Rab Ypt32 interacts with two GAPs, Gyp1 and Gyp6, and may thus control Rab activity at the *trans*-Golgi network. Ypt32 is required for the stability and activity of Gyp1 to inactivate Ypt1 (Rivera-Molina and Novick, 2009), whereas it seems to target the GAP Gyp6 to promote GTP hydrolysis of Ypt6 (Suda *et al.*, 2013). Likewise, two GAPs in metazoan cells, RutBC1 and RutBC2, interact with Rab9-GTP and target Rab32 and Rab36 (Nottingham *et al.*, 2011, 2012). This suggests a general mechanism of Rab control by GAPs that extends also to the endocytic pathway.

Our data did not clarify how BLOC-1 functions at the late endosome. Both BLOC-1 and Mon1-Ccz1 reside on the same organelle, but they do not interact or depend on each other in their localization. On the contrary, BLOC-1 can interact with HOPS at the late endosome and vacuolar membrane and with Ypt7 upon deletion of *msb3*. This Ypt7 interaction could occur via the Ypt7-effector HOPS (Figure 7), because we did not detect significant binding of BLOC1 to Ypt7 in vitro (John Peter *et al.*, 2013). Based on these findings, it nevertheless seems plausible that Vps21 is only inactivated upon fusion of endosomes with vacuoles (Figure 7H). While we show that active Ypt7 is critical for Vps21 inactivation, the exact molecular role of Ypt7 in this cascade is not yet clear. It is possible that free Vps21 only becomes available after it is released from CORVET and retromer (Peplowska *et al.*, 2007; Epp and Ungermann, 2013; Arlt *et al.*, 2015b; Bean *et al.*, 2015). In addition, activated Ypt7 may first engage in retromer-mediated recycling before functioning in fusion or other reactions (Balderhaar *et al.*, 2010; Liu *et al.*, 2012; Figure 7H). Another reason could be that the change in membrane composition that occurs upon fusion with the vacuole is important for Vps21

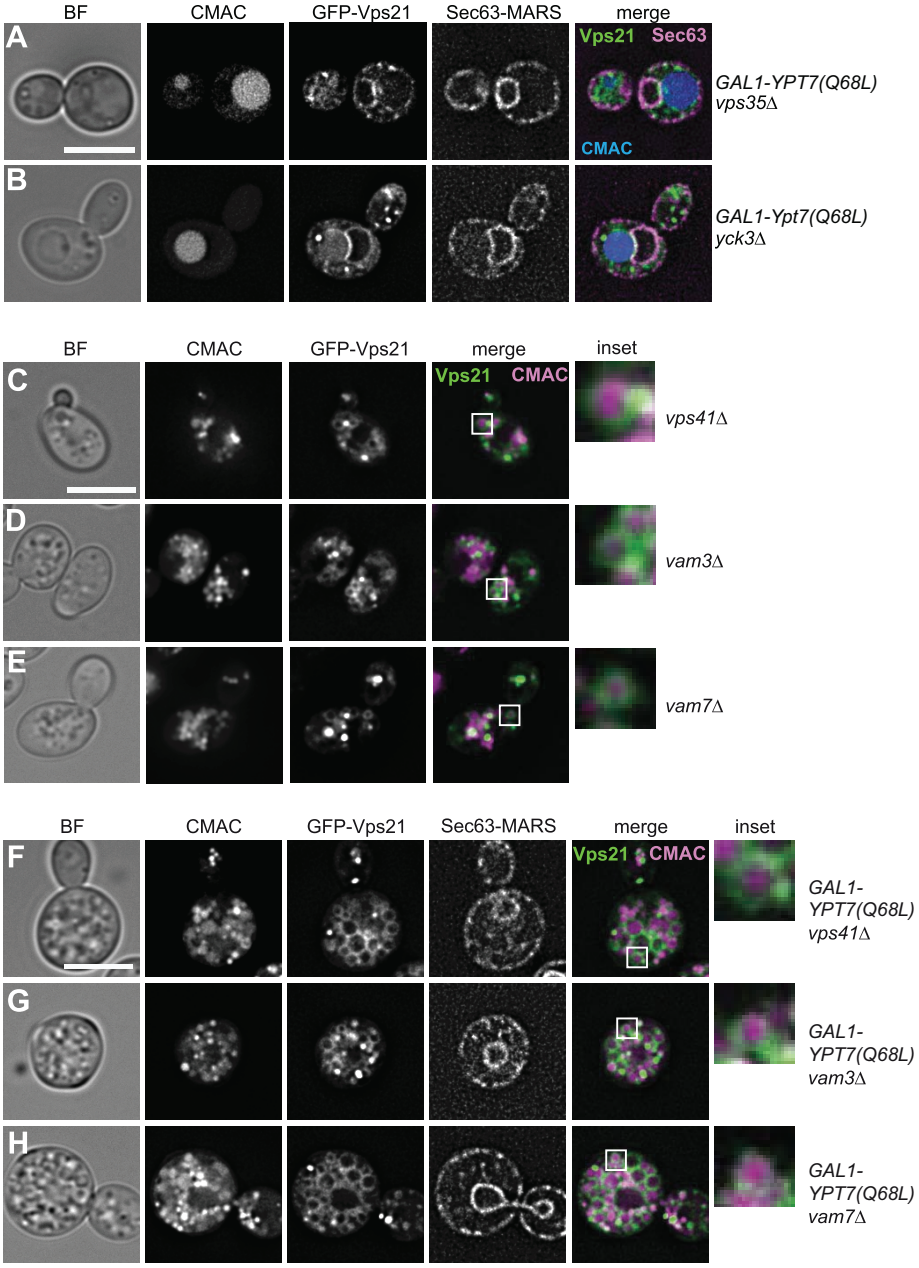

FIGURE 6: The vacuole fusion machinery is required for Vps21 inactivation. (A and B) Effect of deletion of proteins involved in Ypt7-dependent reactions. GFP-Vps21 and Sec63-MARS were coexpressed in cells with overexpressed Ypt7 (Q68L), grown in YPG, and analyzed by fluorescence microscopy. The retromer subunit Vps35 or the casein kinase Yck3 were deleted, where indicated. Vacuoles were stained with CMAC. (C–E) Effect of deletions of the vacuole fusion machinery on Vps21 localization. Deletions of the HOPS subunit Vps41 (C) or the SNAREs Vam3 (D) and Vam7 (E) were analyzed. The vacuolar lumen was stained with CMAC. The area of interest in the white box is enlarged in the inset. (F–H) Localization of GFP-tagged Vps21 in the same deletion strains as in C–E upon Ypt7 (Q68L) overexpression. Markers and analysis were as in A. Cells were analyzed by fluorescence microscopy. The area of interest in the white box is enlarged in the inset. Scale bar: 5 µm.

inactivation and may be accompanied by a conformational change in BLOC-1. We also do not yet know when Msb3 is recruited, because the strong localization of Msb3 at polarized growth sites of the plasma membrane has made it challenging to analyze its localization to endosomes (Lachmann *et al.*, 2012). On BLOC-1 overexpression, Msb3 is found on the vacuolar surface, and an interaction between Ypt7 and Msb3 has also been detected (John Peter *et al.*, 2013). It is possible that Msb3 is recruited via BLOC-1 only upon endosome–vacuole fusion. Future studies will need to address how Ypt7 and HOPS affect BLOC-1 and thus the GAP activity of Msb3. Our reconstitution approach here is a promising start.

In summary, we provide evidence that the GAP activity of Msb3 for Vps21 is controlled by active Ypt7 and its downstream effector HOPS in the context of vacuole fusion. Thus efficient Vps21 inactivation is coupled to endosomal biogenesis, which indicates a conserved principle of Rab control in the endocytic and exocytic pathway.

MATERIALS AND METHODS

Yeast strain construction and molecular biology

The yeast strains used in the present study are listed in Table 1. Tagging, overexpression, and deletion of genes of interest was achieved by homologous recombination of the PCR fragment containing the flanking regions that bind at the 5′ or 3′ end of the gene of interest (Janke *et al.*, 2004). Alternatively, the desired constructs were expressed from a *CEN* plasmid. For the colocalization experiment of Mon1 and Vps21, the dsRed-*VPS21* construct was expressed from a pRS416-*PHO5pr* vector. For Snn1 and Ypt7 colocalization, mCherry-Ypt7 was expressed from pRS416-TPIpr vector (Cabrera and Ungermann, 2013). For epistatic analysis of Msb3 and Ypt7, the yeast strains were transformed with either pRS414-*NOP1pr-YPT7* or pRS414-*NOP1pr-YPT7 K127E* vectors (Cabrera and Ungermann, 2013). All plasmids are listed in Table 2.

Biochemical methods

Purification of overexpressed BLOC-1 via Vab2-TAP (tandem affinity purification) from yeast cells containing or lacking Msb3, and Rab pull-down analyses were done as described (John Peter *et al.*, 2013). BLOC-1 used for GAP assays was purified without detergent (John Peter *et al.*, 2013). Purified FLAG-tagged HOPS and tetrameric AP-3 complexes were provided by Erdal Yavavli and will be described elsewhere (unpublished data).

Fluorescence microscopy

Yeast cells were grown overnight in yeast peptone dextrose (YPD), yeast peptone galactose (YPG), or synthetic complete (SC) medium supplemented with required amino acids and carbon source (for maintenance of transformed plasmids). Cultures grown overnight were diluted in the morning and grown to mid log phase. One milliliter of cells was harvested and resuspended in 50 µl of medium. For 7-amino-4-chloromethylcoumarin (CMAC) staining of the vacuolar lumen, 0.5 µl of CMAC (from 10 µM stock) was added and

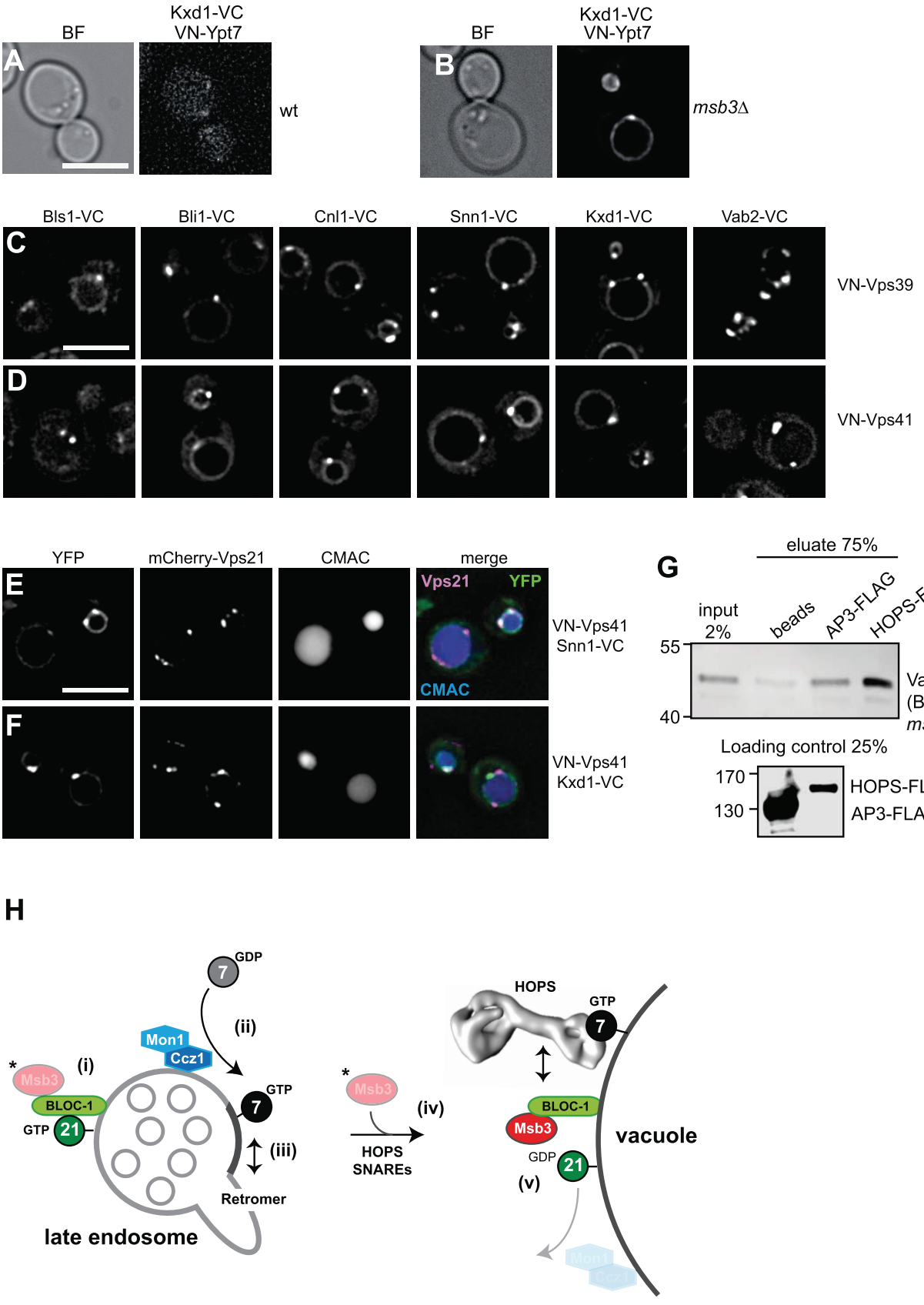

FIGURE 7: BLOC-1 interacts with Ypt7 and the HOPS subunits Vps39 and Vps41 in vivo. (A) Interaction of Ypt7 and BLOC-1 on membranes. VN-Ypt7 and Kxd1-VC were coexpressed in wild-type (A) and *msb3*Δ (B) strains. VN-Ypt7 was under the control of the CET1 promoter. The cells were grown in SDC-URA to maintain the BLOC1-VC–harboring plasmid (A–F), and the expression of BLOC1-VC regulated by the MET25 promoter was induced by growth in

incubated for 15 min at 30°C on a thermomixer. For FM4-64 labeling of the endosomal and vacuolar membranes, 30 µM of FM4-64 was added, and cells were processed as described in Lachmann *et al*. (2012). Cells were harvested and washed with synthetic media and resuspended in 20 µl of media. Cells were mounted on a cover slide, and images were acquired using a Delta Vision Elite (GE Heathcare, Piscataway, NJ) equipped with an inverted microscope (model IX-71; Olympus), an UAPON 100× (1.49 NA) oil-immersion objective or a PLAPON 60× (1.42 NA) oil-immersion objective, an InsightSSI light source (Applied Precision, Issaquah, WA), and an sCMOS camera (PCO, Kehlheim, Germany). Where indicated, z-stacks of 10 sections with 200-nm spacing were subjected to three-dimensional deconvolution using the SoftWoRx 5.5 software and stacked to one image with average intensity. For the rest of the images, one representative plane of a z-stack is shown. For Figure 1A, a Leica DM5500 B microscope equipped with a SPOT Pursuit camera and HCX PL-APO 100× (1.46 NA) oil-immersion objective was used. Pictures were processed using ImageJ (developed by Wayne Rasband, National Institutes of Health, Bethesda, MD) and Adobe Photoshop CS3. The processed images were assembled on Adobe Illustrator CS3.

Split-YFP assay

The split-YFP assay is based on a bimolecular fluorescence complementation system to detect protein–protein interaction in vivo (Sung and Huh, 2007). The plasmids harboring the BLOC-1 subunits with a VC tag (aa 155–238 of Venus) were constructed as described previously (John Peter *et al*., 2013). The N-terminal tagging of Vps21, Vps39, Vps41, and Ypt7 with VN tag (aa 1–154 of Venus) was carried out as previously described (Lachmann *et al*., 2012). The plasmid constructs were transformed into yeast strains harboring genomically VN-tagged proteins and grown in selective medium lacking methionine to express BLOC-1 subunits that were under the control of a *MET25* promoter. An interaction between the tested subunits was visualized as a YFP signal under the fluorescence microscope.

MLV preparation

The MLVs were prepared as previously described (Sot *et al*., 2013). Briefly, a lipid mixture consisting of 55 mol% dioleoylphosphatidylcholine, 20 mol% dioleoylphophatidylethanolamine, 4.4 mol% dioleolyphosphatidylserine, 4.1 mol% dioleoylphosphatidic acid, 1 mol% phosphatidylinositol-3-phosphate, and 15 mol% DOGS-NTA to a final concentration of 6 mM was dried and then rehydrated in buffer (50 mM HEPES/NaOH, pH 7.4, 150 mM NaCl, 1 mg/ml bovine serum albumin [BSA]). The rehydrated mixture was then subjected to nine alternating cycles of freeze and thaw.

GAP assay

The assay was performed according to the protocol described previously (Haas *et al*., 2005). Vps21-His (1 µM) was loaded in 100 µl GTP loading reaction mixture (50 mM HEPES/NaOH, pH 7.4, 150 mM NaCl, 0.5 mM EDTA, 0.05 mM Mg-GTP, 2 µCi γ-[^{32}P] GTP, 1 mg/ml BSA) for 30°C for 15 min. For the experiments conducted on MLVs, the reaction mixtures were incubated for 1 h at 25°C with 0.5 mM MLVs to bind Vps21-His to the liposome surface. The samples were then shifted to ice, and MBP-Msb3 and/or BLOC-1 were added. For BLOC-1 titrations, an internal buffer control was included, such that the final volume was made equal with buffer for all the reactions. The samples were incubated at 30°C for 1 h. The sample (2.5 µl) was directly added to 4 ml of scintillation fluid to calculate the specific activity. Five microliters of the samples in duplicate was added to 0.8 ml of charcoal slurry (5% wt/vol charcoal in 50 mM NaH_2PO_4). The tubes were kept on ice for 1 h to absorb organic phosphates and were centrifuged afterward at 20,000 × *g* for 5 min to pellet the charcoal. A 0.4-ml sample of the supernatant was counted by scintillation (Beckman LS 6000 Liquid Scintillation Counter). The amount of GTP hydrolyzed was calculated as pmoles/hour from the specific activity.

Recombinant protein purification

For purification of recombinant proteins from *E. coli*, cells were grown in 1l LB medium at 37°C to OD_{600} of 0.4–0.7 and then cooled to 16°C, and protein expression was induced by the addition of 0.75 mM isopropyl β-D-1-thiogalactopyranoside. Cells were harvested after overnight growth and were washed once with 100 ml of cold Tris buffer (50 mM Tris, pH 7.4, and 150 mM NaCl) at 3500 × *g* for 10 min. The pellet was resuspended in 15 ml of buffer containing 0.05× PIC (protease inhibitor cocktail; 1x = 0.1 mg/ml of leupeptin, 1 mM *o*-phenanthroline, 0.5 mg/ml of pepstatin A, 0.1 mM Pefabloc) and 1 mM phenylmethylsulfonyl fluoride. Cells were lysed using the Microfluidizer M-110L (Microfluidics, Newton, MA), and the lysate was centrifuged for 30 min at 20,000 × *g* at 4°C. The cleared lysate was incubated with glutathione Sepharose 4B (GE Healthcare), nickel-nitriloacetic acid agarose (Qiagen GmbH, Hilden, Germany), or amylose resin (New England BioLabs, Frankfurt, Germany) for 2 h at 4°C. The resin was washed with 20 column volumes of the buffer, and bound protein was eluted from the respective beads using 20 mM glutathione, 0.3 M imidazole, or 10 mM maltose. The eluted protein was desalted on a PD-10 column using storage buffer (50 mM Tris, pH 7.4, 150 mM NaCl, 5% glycerol), flash frozen, and stored at −80°C in small aliquots.

GST pull down

One hundred micrograms of the purified proteins (GST, GST-Bli1, GST-Cnl1, GST-Snn1, GST-Kxd1, and GST-Vab2) was coupled to

SDC-URA-MET. z-Stacks of 10 sections with 200-nm spacing were stacked to one image with average intensity. Cells were analyzed for YFP fluorescence by microcopy. (C and D) Interaction of HOPS subunits with BLOC-1. VN-Vps39 (C) and VN-Vps41 (D) were coexpressed with C-terminally VC-tagged BLOC-1 subunits (Bls1-VC, Bli1-VC, Cnl1-VC, Snn1-VC, Kxd1-VC, and Vab2-VC). Analysis was as in A. (E and F) Colocalization of interacting HOPS-BLOC-1 with endosomes. mCherry-Vps21 was coexpressed with VN-Vps41 and Snn1-VC (E) or Kxd1-VC (F). Scale bar: 5 µm. (G) BLOC-1 interacts with purified HOPS complex in vitro. Purified BLOC-1 (Vab2-Cbp) from *msb3*Δ cells was incubated for 1 h with FLAG beads, or beads carrying purified AP3-FLAG, and HOPS-FLAG. Bound protein was eluted by boiling with 4× sample buffer. The bound protein was analyzed by Western blotting with an anti-TAP antibody. HOPS-FLAG and AP-3-FLAG were detected by anti-FLAG antibodies. (H) Working model of Vps21 inactivation by BLOC-1 and Msb3. BLOC-1 is initially recruited to the endosome by Vps21-GTP (i). Upon Ypt7 activation by the Mon1-Ccz1 GEF complex (ii), Ypt7-GTP may first interact with retromer (iii) before engaging in fusion (iv). After fusion with the vacuole, Msb3 promotes Vps21 release (v), possibly due to a change in the membrane environment or due to HOPS/Ypt7-mediated stimulation of Msb3. (*) We do not yet know when Msb3 is recruited by BLOC-1. For further discussion, see the main text.

Strain	Genotype	Source
BJ3505	*MATa pep4Δ::HIS3 prb1-Δ1.6R lys2-208 trp1Δ101 ura3-52 gal2*	Haas *et al.*, 1995
BY4727	*MATalpha his3Δ leu2Δ lys2Δ met15Δ trp1Δ ura3Δ*	Euroscarf
BY4732	*MATa his3Δ leu2Δ met15Δ trp1Δ ura3Δ0*	Euroscarf
BY4733	*MATalpha his3Δ200 leu2Δ0 met15Δ0 trp1Δ63 ura3Δ0*	Euroscarf
BY4741	*MATa his3Δ leu2Δ met15Δ ura3Δ0*	Euroscarf
SEY6210	*MATalpha leu2-3112 ura3-52 his3-Δ200 trp-Δ901 lys2-801 suc2-Δ9 GAL*	Robinson *et al.*, 1988
CUY820	BY4741 *YPT7::HIS5-PHO5pr-Myc-GFP*	This study
CUY2349	SEY6210 *MON1::GFP-HIS3*	Nordmann *et al.*, 2010
CUY2696	BY4733 *VPS21::URA3-PHO5pr-GFP*	Markgraf *et al.*, 2009
CUY3276	BY4733 *VPS8::GFP -TRP1*	Markgraf *et al.*, 2009
CUY6741	BY4741 *SNN1::GFP-KanMX*	John Peter *et al.*, 2013
CUY7402	BY4733 X BY4741 *VAB2::natNT2-GAL1pr VAB2::TAP-URA3 CNL1:hphNT1-GAL1pr BLI1::kanMX-GAL1pr SNN1::natNT2-GALpr KXD1::kanMX-GALpr BLS1::hphNT1-GAL1pr*	John Peter *et al.*, 2013
CUY7742	BY4727 *VPS39::HIS3-CET1pr-VN*	Auffarth *et al.*, 2014
CUY7773	SEY6210 *cnl1Δ::natNT2*	This study
CUY7899	SEY6210 *ypt7Δ:natNT2*	This study
CUY8122	SEY6210 *MON1-GFP::HIS3*	This study
CUY8134	SEY6210 *CCZ1-GFP::HIS3*	This study
CUY8262	SEY6210 *msb3Δ::natNT2*	This study
CUY8277	SEY6210 *cnl1Δ::natNT2 ypt7Δ::hphNT1*	This study
CUY8281	SEY6210 *msb3Δ:natNT2 ypt7Δ::hphNT1*	This study
CUY8343	BY4741 *YPT7::HIS5-PHO5pr-Myc-GFP VPS21::natNT2-ADHpr- mCherry*	This study
CUY8633	BY4727 *VPS41::HIS3-CET1pr-VN*	Auffarth *et al.*, 2014
CUY8873	BY4727 *VPS21::KanMX-CET1pr-VN*	This study
CUY9158	BY4741 *VPS21::URA3-PHO5pr-GFP SEC63::MARS-natNT2*	This study
CUY9297	BY4741 *SNN1::GFP-kanMX MON1::MARS-hphNT1*	This study
CUY9352	BY4733 *VPS21::URA3-PHO5pr-GFP ccz1Δ::hphNTI mon1Δ::kanMX*	This study
CUY9424	BY4741 *SNN1::GFP-kanMX mon1Δ::MET15 ccz1Δ::hphNT1*	This study
CUY9426	BY4733 *VPS21::URA3-PHO5pr-GFP ccz1Δ::hphNTI mon1Δ::kanMX msb3Δ::natNT2*	This study
CUY9428	BY4741 *kxd1Δ::hphNT1 YPT7::URA3-PHO5pr-GFP*	This study
CUY9451	BY4741 *kxd1Δ::hphNT1 CCZ1::GFP-kanMX*	This study
CUY9534	BY4741 *URA3-PHO5pr-GFP-myc SEC63::MARS-NatNT2 ypt7Δ::hphNT1*	This study
CUY9535	BY4732 *MON1::HIS3-GAL1pr CCZ1::kanMX-GAL1pr VPS21::URA3-PHO5pr-GFP-myc SEC63::MARS-natNT2*	This study
CUY9540	BY4732 *MON1::HIS3-GAL1pr CCZ1::kanMX-GAL1pr VPS21::URA3-PHO5pr-GFP-myc SEC63::MARS-natNT2 ypt7Δ::hphNT1*	This study
CUY9621	BY4727 *YPT7::kanMX-CET1pr-VN*	This study
CUY9649	BJ3505 *YPT7(Q68L)::kanMX-GAL1pr VPS21::URA3-PHO5pr-VPS21 kxd1Δ::hphNT1 SEC63::MARS-natNT2*	This study
CUY9651	BJ3505 *YPT7(Q68L)::kanMX-GAL1pr VPS21::URA-PHO5pr-VPS21 msb3Δ::hphNT1 SEC63::MARS-natNT2*	This study
CUY9652	BJ3505 *YPT7::kanMX-GAL1pr VPS21::URA3-PHO5pr-GFP SEC63::MARS-natNT2*	This study
CUY9653	BJ3505 *YPT7(Q68L)::kanMX-GAL1pr VPS21::URA-PHO5pr-VPS21 SEC63::MARS-natNT2*	This study
CUY9654	BJ3505 *YPT7(Q68L)::kanMX-GAL1pr VPS21::URA-PHO5pr-VPS21 VPS9::hphNT1-GAL1pr SEC63::MARS-natNT2*	This study
CUY9688	BY4733 X BY4741 *VAB2::natNT2-GAL1pr VAB2::TAP-URA3 CNL1::hphNT1-GAL1pr BLI1::kanMX-GAL1pr msb3Δ::HIS3 SNN1::natNT2-GALpr KXD1::kanMX-GAL1pr BLS1::hphNT1-GALpr msb3Δ::HIS3*	This study

TABLE 1: *Saccharomyces cerevisiae* strains used in this study.

Continues

Strain	Genotype	Source
CUY9725	BJ3505 *YPT7(Q68L)::kanMX-GAL1pr VPS21::URA-PHO5pr-VPS21 SEC63::MARS-natNT2 yck3Δ::hphNT1*	This study
CUY9726	BJ3505 *YPT7(Q68L)::kanMX-GAL1pr VPS21::URA-PHO5pr-VPS21 SEC63::MARS-natNT2 vps35Δ::hphNT1*	This study
CUY9729	BY4733 *VPS8::GFP -TRP1 ccz1Δ::natNT2 mon1Δ::kanMX*	This study
CUY9750	BY4733 *VPS21::URA3-PHO5pr-GFP vam3Δ::hphNT1*	This study
CUY9752	BJ3505 *YPT7(Q68L)::kanMX-GAL1pr VPS21::URA-PHO5pr-VPS21 SEC63::MARS-natNT2 vam3Δ::hphNT1*	This study
CUY9753	BY4733 *VPS21::URA3-PHO5pr-GFP vam7Δ::hphNT1*	This study
CUY9755	BJ3505 *YPT7(Q68L)::kanMX-GAL1pr VPS21::URA-PHO5pr-VPS21 SEC63::MARS-natNT2 vam7Δ::hphNT1*	This study
CUY9756	BY4733 *VPS21::URA3-PHO5pr-GFP vps41Δ::hphNT1*	This study
CUY9758	BJ3505 *YPT7(Q68L)::kanMX-GAL1pr VPS21::URA-PHO5pr-VPS21 SEC63::MARS-natNT2 vps41Δ::hphNT1*	This study
CUY9788	BY4733 *VPS21::URA3-PHO5pr-GFP VPS8::3xmCherry-HIS3*	This study
CUY9789	BY4733 *VPS21::URA3-PHO5pr-GFP ccz1Δ::hphNTI mon1Δ::KanMX VPS8::3xmCherry-HIS3*	This study
CUY9796	BY4727 *VPS41::HIS3-CET1pr-VN VPS21::natNT2-ADHpr-mCherry*	This study
CUY9798	BY4727 *YPT7::kanMX-CET1pr-VN msb3Δ::natNT2*	This study
CUY9905	BJ3505 *YPT7(Q68L) VPS21::URA3-PHO5pr-GFP kxd1Δ::hphNT1*	This study
CUY9906	BJ3505 *YPT7(Q68L) VPS21::URA3-PHO5pr-GFP msb3Δ::hphNT1*	This study

TABLE 1: *Saccharomyces cerevisiae* strains used in this study. Continued

Name	Source
pME3412-*BLS1-VC*	John Peter *et al.*, 2013
pME3412-*BLI1-VC*	John Peter *et al.*, 2013
pME3412-*CNL1-VC*	John Peter *et al.*, 2013
pME3412-*SNN1-VC*	John Peter *et al.*, 2013
pME3412-*KXD1-VC*	John Peter *et al.*, 2013
pME3412-*VAB2-VC*	John Peter *et al.*, 2013
pRS414-*NOP1pr-YPT7*	Cabrera *et al.*, 2013
pRS414-*NOP1pr-YPT7(K127E)*	Cabrera *et al.*, 2013
pRS416-*PHO5pr-dsRED-VPS21*	This study
pRS416-*TPIpr-mCherry-YPT7*	This study
pCDF-*GST-BLI1*	This study
pCDF-*GST-CNL1*	This study
pCDF-*GST-SNN1*	This study
pCDF-*GST-KXD1*	This study
pCDF-*GST-VAB2*	This study
pCOLA-*HIS-SUMO-BLI1*	This study
pCOLA- *HIS-SUMO-CNL1*	This study
pCOLA- *HIS-SUMO-SNN1*	This study
pCOLA- *HIS-SUMO-KXD1*	This study
pCOLA- *HIS-SUMO-VAB2*	This study
pMAL-*TEV-MSB3*	Lachmann *et al.*, 2012
pET24b-*VPS21*	This study
pETGEX-*VAB2-GST*	This study
pFAT2-*HIS-GST-VPS21*	Baldehaar *et al.*, 2013
pFAT2-*HIS-GST-YPT7*	Baldehaar *et al.*, 2013

TABLE 2: Plasmids used in this study.

50 µl of prewashed (wash buffer: 20 mM HEPES/NaOH, pH 7.4, 150 mM NaCl, 2 mM $MgCl_2$, 0.1% TX-100, 7 mg/ml BSA, 5 mM β-mercaptoethanol) glutathione Sepharose 4B (GE Healthcare) beads for 1 h at 4°C. After coupling, the beads were again washed and incubated with 20 µg purified MBP-Msb3 or His-SUMO–tagged recombinant BLOC-1 subunits at 4°C for 2 h. Afterward, the beads were pelleted and washed with the buffer three times to remove protein unspecifically bound to the resin. The bound protein was eluted by boiling with 40 µl of 4× SDS sample buffer, separated by SDS–PAGE, and detected by Western blotting with anti-His or MBP antibodies. Five microliters of the eluate were separated by SDS–PAGE and stained with Coomassie to monitor the equal loading.

ACKNOWLEDGMENTS

We thank Lars Langemeyer for critical feedback, Margarita Cabrera and Arun Thomas John Peter for advice and support, Erdal Yavavli for providing purified HOPS-FLAG and AP3-FLAG protein complexes, and Helmut Wieczorek and Olga Vitavska for support with the GAP assays. This work was supported by a mobility stipend of the Boehringer Ingelheim Foundation (to M.R.) and the Deutsche Forschungsgemeinschaft, Sonderforschungsbereich (SFB) 944, project P11. C.U. is also supported by the Hans-Mühlenhoff Foundation.

REFERENCES

Ali BR, Wasmeier C, Lamoreux L, Strom M, Seabra MC (2004). Multiple regions contribute to membrane targeting of Rab GTPases. J Cell Sci 117, 6401–6412.

Arlt H, Auffarth K, Kurre R, Lisse D, Piehler J, Ungermann C (2015a). Spatio-temporal dynamics of membrane remodeling and fusion proteins during endocytic transport. Mol Biol Cell 26, 1357–1370.

Arlt H, Reggiori F, Ungermann C (2015b). Retromer and the dynamin Vps1 cooperate in the retrieval of transmembrane proteins from vacuoles. J Cell Sci 128, 645–655.

Auffarth K, Arlt H, Lachmann J, Cabrera M, Ungermann C (2014). Tracking of the dynamic localization of the Rab-specific HOPS subunits reveal their distinct interaction with Ypt7 and vacuoles. Cell Logistics 4, e29191.

Balderhaar HJK, Arlt H, Ostrowicz CW, Bröcker C, Sündermann F, Brandt R, Babst M, Ungermann C (2010). The Rab GTPase Ypt7 is linked to retromer-mediated receptor recycling and fusion at the yeast late endosome. J Cell Sci 123, 4085–4094.

Balderhaar HJK, Lachmann J, Yavavli E, Bröcker C, Lürick A, Ungermann C (2013). The CORVET complex promotes tethering and fusion of Rab5/Vps21-positive membranes. Proc Natl Acad Sci USA 110, 3823–3828.

Balderhaar HJK, Ungermann C (2013). CORVET and HOPS tethering complexes—coordinators of endosome and lysosome fusion. J Cell Sci 126, 1307–1316.

Barr F, Lambright DG (2010). Rab GEFs and GAPs. Curr Opin Cell Biol 22, 461–470.

Barr FA (2013). Rab GTPases and membrane identity: causal or inconsequential? J Cell Biol 202, 191–199.

Bean BDM, Davey M, Snider J, Jessulat M, Deineko V, Tinney M, Stagljar I, Babu M, Conibear E (2015). Rab5-family guanine nucleotide exchange factors bind retromer and promote its recruitment to endosomes. Mol Biol Cell 26, 1119–1128.

Bröcker C, Kuhlee A, Gatsogiannis C, Kleine Balderhaar HJ, Hönscher C, Engelbrecht-Vandré S, Ungermann C, Raunser S (2012). Molecular architecture of the multisubunit homotypic fusion and vacuole protein sorting (HOPS) tethering complex. Proc Natl Acad Sci USA 109, 1991–1996.

Cabrera M, Arlt H, Epp N, Lachmann J, Griffith J, Perz A, Reggiori F, Ungermann C (2013). Functional separation of endosomal fusion factors and the class C core vacuole/endosome tethering (CORVET) complex in endosome biogenesis. J Biol Chem 288, 5166–5175.

Cabrera M, Langemeyer L, Mari M, Rethmeier R, Orban I, Perz A, Bröcker C, Griffith J, Klose D, Steinhoff H-J, *et al*. (2010). Comment on: phosphorylation of a membrane curvature-sensing motif switches function of the HOPS subunit Vps41 in membrane tethering. J Cell Biol 191, 845–859.

Cabrera M, Nordmann M, Perz A, Schmedt D, Gerondopoulos A, Barr F, Piehler J, Engelbrecht-Vandré S, Ungermann C (2014). The Mon1-Ccz1 GEF activates the Rab7 GTPase Ypt7 via a longin-fold-Rab interface and association with PI3P-positive membranes. J Cell Sci 127, 1043–1051.

Cabrera M, Ungermann C (2013). Guanine nucleotide exchange factors (GEFs) have a critical but not exclusive role in organelle localization of Rab GTPases. J Biol Chem 288, 28704–28712.

del Conte-Zerial P, Brusch L, Rink JC, Collinet C, Kalaidzidis Y, Zerial M, Deutsch A (2008). Membrane identity and GTPase cascades regulated by toggle and cut-out switches. Mol Syst Biol 4, 206.

Di Pietro SM, Falcón-Pérez JM, Tenza D, Setty SRG, Marks MS, Raposo G, Dell'Angelica EC (2006). BLOC-1 interacts with BLOC-2 and the AP-3 complex to facilitate protein trafficking on endosomes. Mol Biol Cell 17, 4027–4038.

Epp N, Ungermann C (2013). The N-terminal domains of Vps3 and Vps8 are critical for localization and function of the CORVET tethering complex on endosomes. PLoS One 8, e67307.

Gao X-D, Albert S, Tcheperegine SE, Burd CG, Gallwitz D, Bi E (2003). The GAP activity of Msb3p and Msb4p for the Rab GTPase Sec4p is required for efficient exocytosis and actin organization. J Cell Biol 162, 635–646.

Gautreau A, Oguievetskaia K, Ungermann C (2014). Function and regulation of the endosomal fusion and fission machineries. CSH Perspect Biology 6, a016832.

Haas A (1995). A quantitative assay to measure homotypic vacuole fusion in vitro. Methods Cell Sci 17, 283–294.

Haas AK, Fuchs E, Kopajtich R, Barr FA (2005). A GTPase-activating protein controls Rab5 function in endocytic trafficking. Nat Cell Biol 7, 887–893.

Hayes MJ, Bryon K, Satkurunathan J, Levine TP (2011). Yeast homologues of three BLOC-1 subunits highlight KxDL proteins as conserved interactors of BLOC-1. Traffic 12, 260–268.

Huotari J, Helenius A (2011). Endosome maturation. EMBO J 30, 3481–3500.

Hutagalung AH, Novick PJ (2011). Role of Rab GTPases in membrane traffic and cell physiology. Physiol Rev 91, 119–149.

Itzen A, Goody RS (2011). GTPases involved in vesicular trafficking: structures and mechanisms. Semin Cell Dev Biol 22, 48–56.

Janke C, Magiera MM, Rathfelder N, Taxis C, Reber S, Maekawa H, Moreno-Borchart A, Doenges G, Schwob E, Schiebel E, *et al*. (2004). A versatile toolbox for PCR-based tagging of yeast genes: new fluorescent proteins, more markers and promoter substitution cassettes. Yeast 21, 947–962.

John Peter AT, Lachmann J, Rana M, Bunge M, Cabrera M, Ungermann C (2013). The BLOC-1 complex promotes endosomal maturation by recruiting the Rab5 GTPase-activating protein Msb3. J Cell Biol 201, 97–111.

Kucharczyk R, Kierzek AM, Slonimski PP, Rytka J (2001). The Ccz1 protein interacts with Ypt7 GTPase during fusion of multiple transport intermediates with the vacuole in *S. cerevisiae*. J Cell Sci 114, 3137–3145.

Lachmann J, Barr FA, Ungermann C (2012). The Msb3/Gyp3 GAP controls the activity of the Rab GTPases Vps21 and Ypt7 at endosomes and vacuoles. Mol Biol Cell 23, 2516–2526.

Lachmann J, Ungermann C, Engelbrecht-Vandré S (2011). Rab GTPases and tethering in the yeast endocytic pathway. Small GTPases 2, 182–186.

LaGrassa TJ, Ungermann C (2005). The vacuolar kinase Yck3 maintains organelle fragmentation by regulating the HOPS tethering complex. J Cell Biol 168, 401–414.

Lee HH, Nemecek D, Schindler C, Smith WJ, Ghirlando R, Steven AC, Bonifacino JS, Hurley JH (2012). Assembly and architecture of biogenesis of lysosome-related organelles complex-1 (BLOC-1). J Biol Chem 287, 5882–5890.

Liu T-T, Gomez TS, Sackey BK, Billadeau DD, Burd CG (2012). Rab GTPase regulation of retromer-mediated cargo export during endosome maturation. Mol Biol Cell 23, 2505–2515.

Markgraf DF, Ahnert F, Arlt H, Mari M, Peplowska K, Epp N, Griffith J, Reggiori F, Ungermann C (2009). The CORVET subunit Vps8 cooperates with the Rab5 homolog Vps21 to induce clustering of late endosomal compartments. Mol Biol Cell 20, 5276–5289.

Nickerson DP, Russell MRG, Lo S-Y, Chapin HC, Milnes JM, Merz AJ (2012). Termination of isoform-selective Vps21/Rab5 signaling at endolysosomal organelles by Msb3/Gyp3. Traffic 13, 1411–1428.

Nordmann M, Cabrera M, Perz A, Bröcker C, Ostrowicz CW, Engelbrecht-Vandré S, Ungermann C (2010). The Mon1-Ccz1 complex is the GEF of the late endosomal Rab7 homolog Ypt7. Curr Biol 20, 1654–1659.

Nottingham RM, Ganley IG, Barr FA, Lambright DG, Pfeffer SR (2011). RUTBC1 protein, a Rab9A effector that activates GTP hydrolysis by Rab32 and Rab33B proteins. J Biol Chem 286, 33213–33222.

Nottingham RM, Pusapati GV, Ganley IG, Barr FA, Lambright DG, Pfeffer SR (2012). RUTBC2 protein, a Rab9A effector and GTPase-activating protein for Rab36. J Biol Chem 287, 22740–22748.

Ostrowicz CW, Bröcker C, Ahnert F, Nordmann M, Lachmann J, Peplowska K, Perz A, Auffarth K, Engelbrecht-Vandré S, Ungermann C (2010). Defined subunit arrangement and Rab interactions are required for functionality of the HOPS tethering complex. Traffic 11, 1334–1346.

Peplowska K, Markgraf DF, Ostrowicz CW, Bange G, Ungermann C (2007). The CORVET tethering complex interacts with the yeast Rab5 homolog Vps21 and is involved in endo-lysosomal biogenesis. Dev Cell 12, 739–750.

Plemel RL, Lobingier BT, Brett CL, Angers CG, Nickerson DP, Paulsel A, Sprague D, Merz AJ (2011). Subunit organization and Rab interactions of Vps-C protein complexes that control endolysosomal membrane traffic. Mol Biol Cell 22, 1353–1363.

Poteryaev D, Datta S, Ackema K, Zerial M, Spang A (2010). Identification of the switch in early-to-late endosome transition. Cell 141, 497–508.

Rak A, Pylypenko O, Durek T, Watzke A, Kushnir S, Brunsveld L, Waldmann H, Goody RS, Alexandrov K (2003). Structure of Rab GDP-dissociation inhibitor in complex with prenylated YPT1 GTPase. Science 302, 646–650.

Rink J, Ghigo E, Kalaidzidis Y, Zerial M (2005). Rab conversion as a mechanism of progression from early to late endosomes. Cell 122, 735–749.

Rivera-Molina FE, Novick PJ (2009). A Rab GAP cascade defines the boundary between two Rab GTPases on the secretory pathway. Proc Natl Acad Sci USA 106, 14408–14413.

Robinson JS, Klionsky DJ, Banta LM, Emr SD (1988). Protein sorting in Saccharomyces cerevisiae: isolation of mutants defective in the delivery and processing of multiple vacuolar hydrolases. Mol Cell Biol 8, 4936–4948.

Rojas R, van Vlijmen T, Mardones GA, Prabhu Y, Rojas AL, Mohammed S, Heck AJ, Raposo G, van der Sluijs P, Bonifacino JS (2008). Regulation of retromer recruitment to endosomes by sequential action of Rab5 and Rab7. J Cell Biol 183, 513–526.

Salazar G, Craige B, Styers ML, Newell-Litwa KA, Doucette MM, Wainer BH, Falcon-Perez JM, Dell'Angelica EC, Peden AA, Werner E, *et al*. (2006). BLOC-1 complex deficiency alters the targeting of adaptor protein complex-3 cargoes. Mol Biol Cell 17, 4014–4026.

Seals D, Eitzen G, Margolis N, Wickner W, Price A (2000). A Ypt/Rab effector complex containing the Sec1 homolog Vps33p is required for homotypic vacuole fusion. Proc Natl Acad Sci USA 97, 9402–9407.

Setty SRG, Tenza D, Truschel ST, Chou E, Sviderskaya EV, Theos AC, Lamoreux ML, Di Pietro SM, Starcevic M, Bennett DC, *et al*. (2007). BLOC-1

is required for cargo-specific sorting from vacuolar early endosomes toward lysosome-related organelles. Mol Biol Cell 18, 768–780.
Singh MK, Krüger F, Beckmann H, Brumm S, Vermeer JEM, Munnik T, Mayer U, Stierhof Y-D, Grefen C, Schumacher K, *et al*. (2014). Protein delivery to vacuole requires SAND protein-dependent Rab GTPase conversion for MVB-vacuole fusion. Curr Biol 24, 1383–1389.
Solinger JA, Spang A (2014). Loss of the Sec1/Munc18-family proteins VPS-33.2 and VPS-33.1 bypasses a block in endosome maturation in *Caenorhabditis elegans*. Mol Biol Cell 25, 3909–3925.
Sot B, Behrmann E, Raunser S, Wittinghofer A (2013). Ras GTPase activating (RasGAP) activity of the dual specificity GAP protein Rasal requires colocalization and C2 domain binding to lipid membranes. Proc Natl Acad Sci USA 110, 111–116.
Suda Y, Kurokawa K, Hirata R, Nakano A (2013). Rab GAP cascade regulates dynamics of Ypt6 in the Golgi traffic. Proc Natl Acad Sci USA 110, 18976–18981.
Sung M-K, Huh W-K (2007). Bimolecular fluorescence complementation analysis system for in vivo detection of protein-protein interaction in *Saccharomyces cerevisiae*. Yeast 24, 767–775.
Wurmser AE, Sato TK, Emr SD (2000). New component of the vacuolar class C-Vps complex couples nucleotide exchange on the Ypt7 GTPase to SNARE-dependent docking and fusion. J Cell Biol 151, 551–562.